8th European Workshop On Structural Health Monitoring (EWSHM 2016), 5-8 July 2016, Spain, Bilbao
www.ndt.net/app.EWSHM2016

Fiber-Optic Based HUMS Concept for Large Aircraft Structure Based on Both Point and Distributed Strain Sensing

Moshe TUR[1], Matthijs B. BOSBOOM[2], Rolf EVENBLIJ[3], Pavlos MICHAELIDES[4], Nahum GORBATOV[1], Arik BERGMAN[1], Uri BEN-SIMON[5], Iddo KRESSEL[5], Nikoalos KONTIS[6], Christos KOIMTZOGLOU[6]

[1]Tel-Aviv University, Tel-Aviv, Israel 69978 tur@post.tau.ac.il
[2]KVE Composite Structures BV, The Hague, 2497GB, The Netherlands, bosboom@kve.nl
[3] Technobis Fibre Technology, Alkmaar, 1812SC, The Netherlands, rolf.evenblij@technobis.com
[4]NAsTech – Novel Aerospace Technologies, Ancarano, 64010, Italy, p.michaelides@nastech.it
[5] Israel Aerospace Industries, Israel, ikressel@iai.co.il
[6]Integrated Aerospace Sciences Corporation – INASCO, Greece, c.koimtzoglou@inasco.com

Key words: Smart structures, FBG, Rayleigh backscattering distributed strain sensing.

Abstract

A hybrid, low cost HUMS concept, based on fiber-optic point and distributed strain sensing for both usage monitoring and damage detection, is presented. Sensing is based on in-flight Fiber Bragg Grating (FBG) technology, combined with on-ground Rayleigh-backscattering distributed strain sensing. The in-flight FBG instrumentation monitors loads and damage at highly critical discrete locations while the Rayleigh-based technique is used on-ground to track damages by monitoring the overall strain signature change on large components, at rest or under prescribed loading, over time. These two sensing concepts were verified on a typical commercial aircraft fuselage stiffened skin panel. The test contained two stages: at first, the panel was impacted near the stiffening stringer, while at the second stage the panel was loaded in compression up to failure. Strain measurements at a spatial resolution of 1.0 cm were recorded during the two test stages. At the same time, FBG strain readings were recorded too. It was clearly observed that the damage done by the impact to the stringer-skin bonding attachment could be traced by the two sensing concepts. It should be noted that measurements were performed after the impact so that the observed traces indicated a permanent effect. The effect of the impact on the strain distribution under static loading, eventually leading to failure, was also tracked. Numerical simulation was performed in order to evaluate the damage effect on the panel residual strength. It is expected that such data may lead to a good numerical prediction of the structure residual strength in the presence of damage, thereby improving aircraft design.

1 INTRODUCTION

This paper presents the application of fiber optic strain sensing to commercial aircraft composite fuselage panels for load monitoring and impact detection. This work is part of the EU SARISTU project aimed at enhancing the technology of Smart Intelligent Aircraft Structures [1]. One aspect of Smart Intelligent Aircraft Structures is applying Structural Health Monitoring (SHM) using Fiber Optic Sensors (FOSs) [2]. Such SHM systems should prove extremely important in composite-made aircraft structure, where conventional inspection methods of critical structural components are time consuming and hindered by limited accessibility. Optical fibers are quite flexible and tolerant to environmental conditions and electromagnetic interferences. In addition, their small diameter allows them to be easily embedded within or externally bonded on large composite structural components, such as wings or fuselage skins, at relatively low cost.

On-ground and In-flight-capable discrete strain measurements using ribbon-tape embedded Fiber Bragg Grating (FBG) [3] based sensor net were successfully applied, demonstrating the reliability and maturity of this technique [2, 4, 5]. For such a concept, any damage not within the spatial sensing range of the individual FBGs cannot be traced. The Rayleigh backscattering distributed strain sensing [6, 7, 8] is a very effective technique for high spatial resolution (sub-centimeter) strain measurements that can overcome the point sensing FBG-based concept. It uses coherent techniques to record the optical magnitude and phase of the Rayleigh backscattering, originating from the random spatial variations of the refractive index in the amorphous glass. This sensing concept was applied to a typical aircraft fuselage skin panel with Omega shaped stringers, tested under compression. A barely-visible impact was introduced at a critical stringer-to-skin joint. Such a damage, if undetected, may have a major influence on the residual strength of such structure.

While the discrete FBGs can track the general loads and dynamic events [8, 9, 10] (impacts, vibrations) of the structure, the rather static Rayleigh backscattering sensing concept can successfully detect the change in strain, originating from a relatively small impact, namely: it can discover an impact-induced damage without the need to capture the impact event. This should pave the way for real time damage detection of large scale composite structures

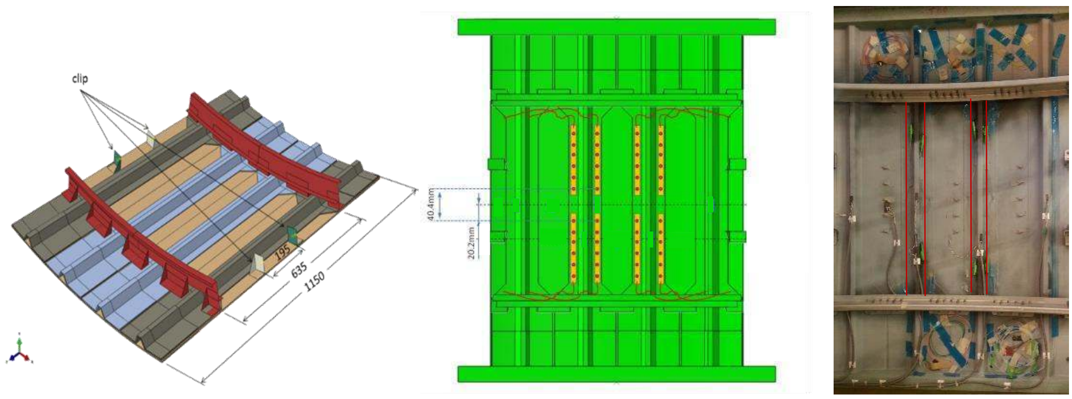

Figure 1: Generic composite A/C fuselage panel: Left – Design; Middle: Schematic with the 4 ribbon tapes, each with 6 FBGs; Right: Complete painted part with the designated locations (4 vertical lines) of the standard polyimide coated single mode fibers used for the distributed sensing.

2 THE SENSING CONCEPT OF IMPACT-INDUCED DAMAGE

A typical aircraft fuselage composite stiffened skin panel was selected for demonstrating both the point and distributed sensing concepts (Fig. 1). FBGs were first embedded in specially designed and manufactured connectorized ribbon tapes [11], 6 FBGs in each tapes. These ribbon tape were designed as a supportive carrier for the optical fiber, which can be co-cured or secondary bonded to the structure. The FBGs served real time dynamic measurements during both the impact test and loading to failure (Fig. 2). The Fiber-optic Rayleigh-backscattering-based sensing concept was applied to a single strand of standard (untreated-no fiber Bragg gratings) optical fiber, which was routed along the full length of the feet of the two middle stringers (Fig. 1, right). Thus, it could cover all events along its route.

Structural integrity is assessed based on: (i) The absence of residual strain after impact; (ii) The stability of the strain signature under loading; and (iii) The linearity of strain readings with respect to the loading. The panel was tested at Imperial College London during April 2015. The test included two stages. At first the specimen, fixed to a rig, was impacted twice near the stringer as shown in Figure 2. At the second stage the panel was compressively loaded up to failure. Strain measurements at a spatial resolution of 1.0 cm were periodically recorded during the two test stages. Typical results for the impact test are shown in the Figure 3 below.

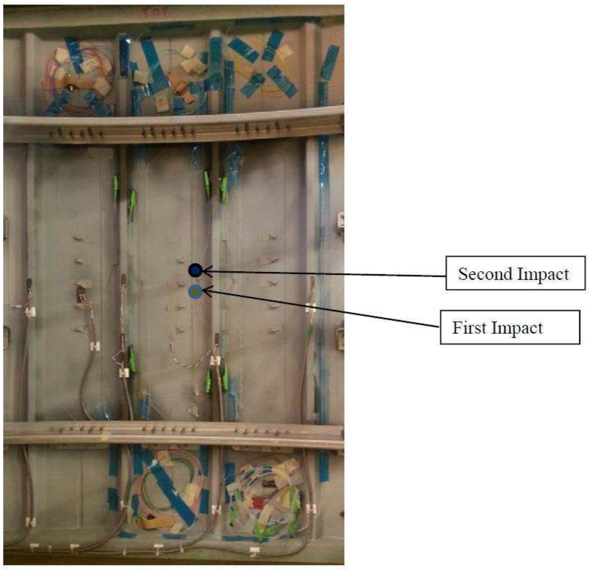

Figure 2: The stiffened skin panel, showing the locations of the barely visible impacts (The impact was performed on the outer side)

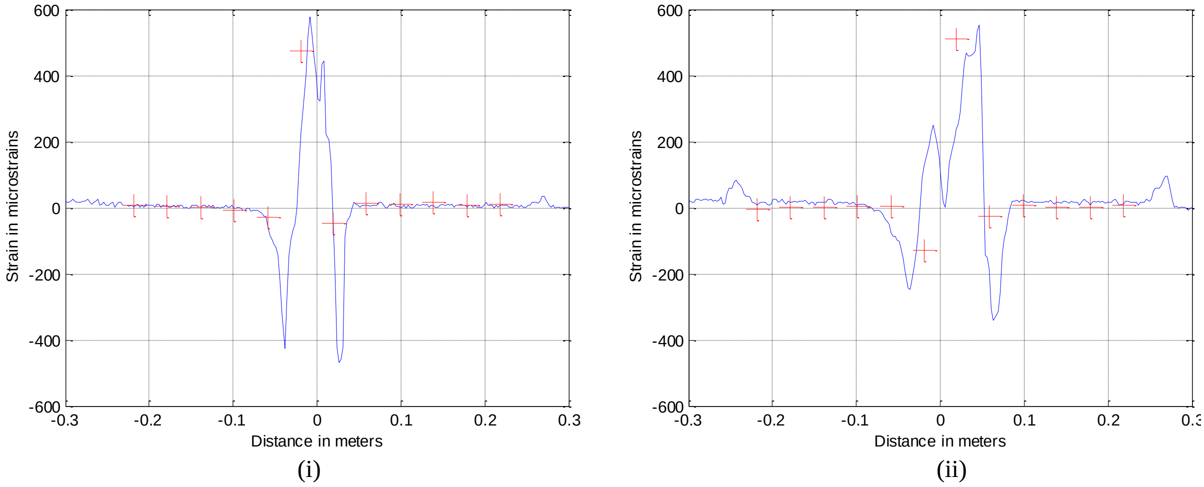

Figure 3: Impact test results. Rayleigh Backscattering distributed Strain Sensing (solid continuous line) and FBG point readings (+), measured after each impact test. The pre-impacts state was used as a reference. (i) First impact, (ii) second impact. The interrogator was Luna OBR4600 on courtesy loan from Luna Innovations Incorporated. The high speed FBG interrogator (20 kHz of sampling rate) is a product of Technobis Fibre Technology.

It is clearly seen (Fig 3) that the damage done by the impact to the stinger-skin bonding attachment can be traced. It should be noted that the measurements reported here were performed after the impact so that the observed traces indicate a permanent effect. The time evolution of the damage (not shown) was traced by the FBGs but not by the static Rayleigh-based technology.

3 RESIDUAL STRENGTH TEST

The effect of the impact on the strain distribution during static loading, eventually leading to failure (not shown) can be seen in Figure 4. Strain distribution at two locations are presented: (i) along an undamaged stringer and (ii) along the stringer with impact damage. This measurement was taken with reference to the impacted panel. Thus, the reference reading, serving as the baseline "0" state, contains all the residual stresses originating from the impact, so that at zero loading the readings should be zero. It is clearly seen that the impact damage caused a significant strain change, which increased with the external load. Specifically, while areas of the panel away from the damage developed strain approximately in proportion to the applied load, the damaged region behaved quite differently. We may say that already at 139KN there are clear signs of local buckling failure.

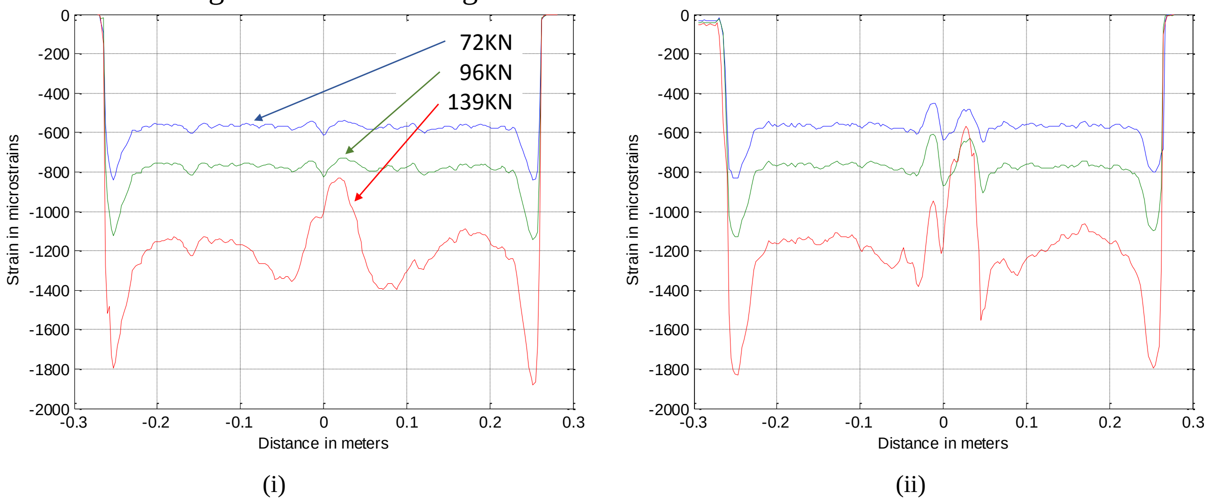

Figure 4: Static loading of the impacted panel: effect of impact on strain distribution along the stringer feet for (i) undamaged stringer and (ii) stringer with impact damage

4 FINITE ELEMENT ANALISIS

The FE model design is depicted in Figure 4, presenting also the extent and locations of the simulated debondings (pink areas). The model is constructed with shell elements where the debonded areas have been represented by simply removing the bonding between stringer and skin at the desired area. More specifically, the panel structure is simulated under six health states: one healthy and five under damage comprising single or multiple debondings. In the current analysis, only three damage cases are considered (see the corresponding figure), namely damage case II, III, and VII, also referred to as damage cases 1, 2, and 3 respectively. The FEA simulation results comprise the strain values at the stringer feet. More precisely, results refer to the right foot of the first stringer (from left to right in Figure 5), both feet of the second and third stringers, and the left foot of the fourth stringer. The naming of the stringers is constituted by the stringer number (1 – 4 from left to right) followed by an underscore and an index indicating the left (1) or right (2) foot. Hence the stringer feet for which the strain data are extracted are named from left to right of Figure 5 as: 1_2, 2_1, 2_2, 3_1, 3_2, and 4_1.

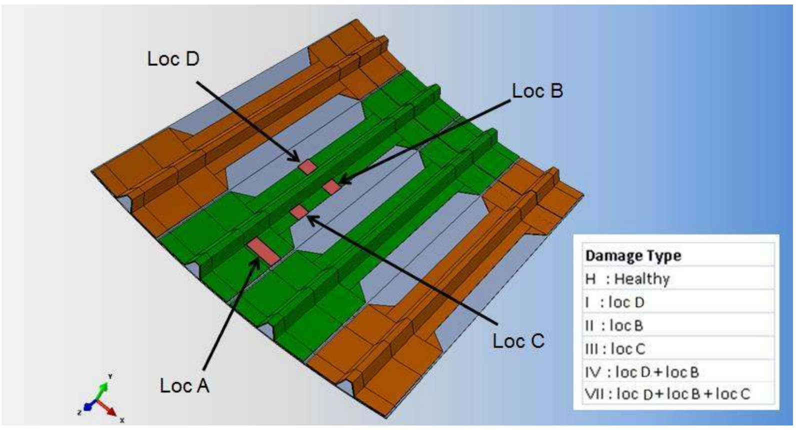

Figure 5. The FE model with the locations of the debondings, and all the simulated damage cases.

The raw strain data at the stringer feet as extracted by the FEM are shown in Figure 6, which contains 6 subplots corresponding to the six stringer feet. In each subplot four lines are drawn corresponding to each structural health state: healthy and damage types II, III, and VII. When damage is present, the debonding area is highlighted by a green strip.

The conclusions that may be drawn from the raw strain data presented in the current section are summarized as: The damage effect on the strain readings extends around 50mm, with a 40mm area presenting a potentially detectable change.

In all the damage cases, strain measurements fluctuate around the healthy ones. Only the stringers that contain the damage are affected by it, whereas the rest ones do not seem to be affected.

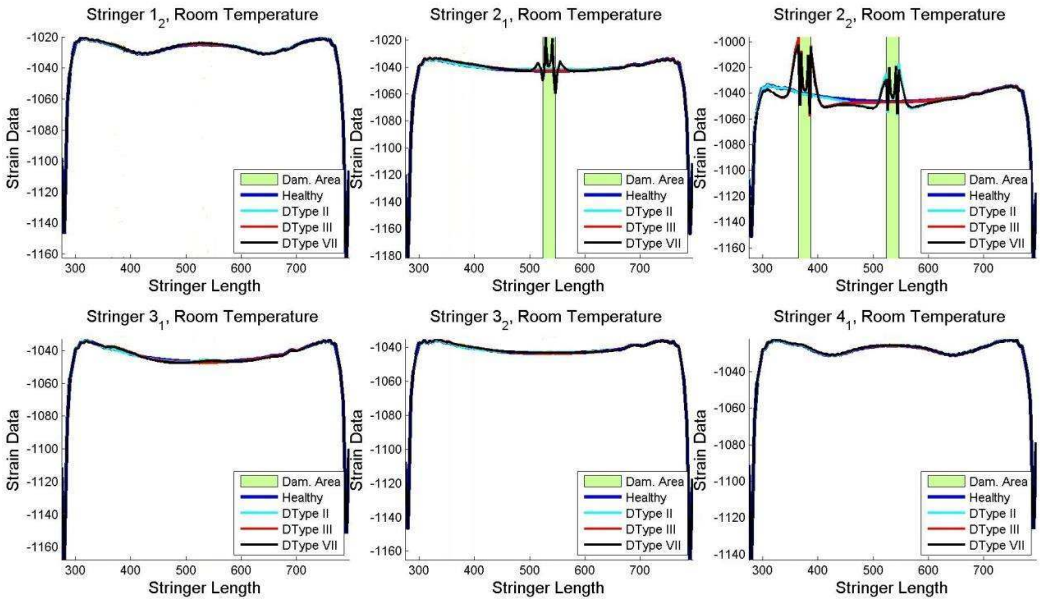

Figure 6. FEA strain data at room temperature, for all damage cases. Blue lines indicate healthy structure, while cyan, red and black lines indicate damage case II, III, and VII respectively. The green areas correspond to debonding locations.

5 CONCLUSIONS

Applying this monitoring concept, where incidental impact with known residual strength can be tracked at short inspections intervals, may lead to weight saving without compromising damage tolerance certification requirements. Integrating this sensing network on real aircraft structure, like wing or fuselage stiffened panels was demonstrated, together with a contribution to the qualification and certification requirements. It must be pointed out that work related to embedded optical fibers sensors, have an added complexity for both manufacturing and interpretation of the sensor response. Nevertheless the approach of applying FOS as demonstrated, in terms of low cost manufacturing and robustness, is a step forward towards the maturation of optical fibers sensing technology for large composite structures application.

6 ACKNOWLEDGMENT

This project has received funding from the European Union's Seventh Framework Programme for research, technological development and demonstration under grant agreement no. 284562. The impact tests and compression experiments were conducted by the ICL group, by Dr. Spyridon Psarras and his highly professional team. Their hospitality and contributions are highly appreciated.

REFERENCES

[1] Farrar, C. R., & Worden, K. (2007). An introduction to structural health monitoring. Philosophical Transactions of the Royal Society of London A: Mathematical, Physical and Engineering Sciences, 365(1851), 303-315.

[2] Todd, M. D., Nichols, J. M., Trickey, S. T., Seaver, M., Nichols, C. J., & Virgin, L. N. (2007). Bragg grating-based fibre optic sensors in structural health monitoring. Philosophical Transactions of the Royal Society of London A: Mathematical, Physical and Engineering Sciences, 365(1851), 317-343.

[3] Othonos, A., & Kalli, K. (1999). Fiber Bragg gratings: fundamentals and applications in telecommunications and sensing. Artech House.

[4] Richards, W.L., Madaras, E., Prosser, W.H., & Studor, G., "NASA Applications of Structural Health Monitoring Technology" 9th International Workshop on Structural Health Monitoring, September 10–12, 2013.

[5] Tsutsui, H., Kawamata, A., Sanda, T., & Takeda, N. (2004). Detection of impact damage of stiffened composite panels using embedded small-diameter optical fibers. Smart Materials and Structures, 13(6), 1284.

[6] Froggatt, M., & Moore, J. (1998). High-spatial-resolution distributed strain measurement in optical fiber with Rayleigh scatter. Applied Optics, 37(10), 1735-1740.

[7] Soller, Brian, et al. "High resolution optical frequency domain reflectometry for characterization of components and assemblies." Optics Express 13.2 (2005): 666-674.

[8] Kressel, I., Dorfman, B., Botsev, Y., Handelman, A., Balter, J., Pillai, A.C.R., M H Prasad, N. Gupta, A M Joseph, R Sundaram, M. Tur, (2015) Flight validation of an embedded structural health monitoring system for an unmanned aerial vehicle. Smart Mat. & Struc., 24(7), 075022.

[9] Güemes, Alfredo, et al. "Methodologies for the Damage Detection Based on Fiber-Optic Sensors. Applications to the Fuselage Panel and Lower Wing Panel." Smart Intelligent Aircraft Structures (SARISTU). Springer International Publishing, 2016. 407-431.

[10] M. Tur, et al. "Structural health monitoring of composite-based UAVs using simultaneous fiber optic interrogation by static Rayleigh-based distributed sensing and dynamic fiber Bragg grating point sensors." (OFS24). International Society for Optics and Photonics, 2015.

[11] Bosboom, Matthijs, et al. "Ribbon Tapes, Shape Sensors, and Hardware. "Smart Intelligent Aircraft Structures (SARISTU). Springer International Publishing, 2016. 349-406